

Electronic Supplementary Information for

## **Monomorphic Platinum Octapod and Tripod Nanocrystals Synthesized by Iron Nitrate Modified Polyol Process**

Jie Yin<sup>a,b</sup>, Junhu Wang<sup>a,c\*□</sup>, Yanjie Zhang<sup>a</sup>, Huanqiao Li<sup>d</sup>, Yujiang Song<sup>d</sup>, Changzi Jin<sup>a</sup>, Ting Lu<sup>a</sup>  
and Tao Zhang<sup>a,c\*</sup>

<sup>a</sup> State Key Laboratory of Catalysis, Dalian Institute of Chemical Physics, Chinese Academy of  
Sciences, Dalian 116023, China

<sup>b</sup> Graduate University of Chinese Academy of Sciences, Beijing 100049, China

<sup>c</sup> Mössbauer Effect Data Center, Dalian Institute of Chemical Physics, Chinese Academy of  
Sciences, Dalian 116023, China

<sup>d</sup> Department of Fuel Cells and Batteries & Basic and Strategic Studies for Energy, Dalian National  
Laboratories for Clean Energy, Dalian Institute of Chemical Physics, Chinese Academy of Sciences,  
Dalian 116023, China

Email: [taozhang@dicp.ac.cn](mailto:taozhang@dicp.ac.cn); [wangjh@dicp.ac.cn](mailto:wangjh@dicp.ac.cn)

- Fig. S1 TEM images of Pt NCs synthesized at 160°C for 20 min with different ratios between Fe(NO<sub>3</sub>)<sub>3</sub> and H<sub>2</sub>PtCl<sub>6</sub> (a) 0, (b) 0.02, (c) 0.1, (d) 0.2, (e) 0.4, (f) 1.0, (g) 1.2, (h) 1.6
- Fig. S2 TEM images of Pt Pt NCs synthesized at 5 mM H<sub>2</sub>PtCl<sub>6</sub> and 5 mM Fe(NO<sub>3</sub>)<sub>3</sub> with different temperatures (a)128°C, (b)140°C, (c)160°C, (d)180°C for 3 h
- Fig. S3 TEM images of Pt NCs synthesized at the same temperature (140°C) and the same Pt concentration (5 mM) but with different ratios between Fe(NO<sub>3</sub>)<sub>3</sub> and H<sub>2</sub>PtCl<sub>6</sub> (a) 1.0, (b) 1.2, (c) 1.8, (d) 2.0 for 3 h
- Fig. S4 TEM images of Pt NCs synthesized at the same temperature (140°C) with same ratios between Fe(NO<sub>3</sub>)<sub>3</sub> and H<sub>2</sub>PtCl<sub>6</sub> but at different Pt concentrations (a) 3 mM, (b) 4 mM, (c) 5 mM, (d) 6 mM, (e) 7 mM for 3 h
- Fig. S5 TEM images of the Pt NCs prepared at 5 mM H<sub>2</sub>PtCl<sub>6</sub> and 5 mM Fe(NO<sub>3</sub>)<sub>3</sub> at 140°C with PVP and CTAB, respectively and pictures of the initial colloid solution and the product solutions with and without PVP
- Fig. S6 TEM images of Pt NCs synthesized at the same temperature (140°C) and the same Pt concentration (5 mM) but with different modifier (a) 5 mM Fe(NO<sub>3</sub>)<sub>3</sub>, (b) 5 mM FeCl<sub>3</sub>, (c) 15 mM NaNO<sub>3</sub>, (d) 7.5 mM Cu(NO<sub>3</sub>)<sub>2</sub>
- Fig. S7 X-ray absorption near-edge fine structure spectra of iron species taken from the quenched solutions at different stages of the synthesis process of Pt octapod (5 mM H<sub>2</sub>PtCl<sub>6</sub>, 5 mM Fe(NO<sub>3</sub>)<sub>3</sub>, 140°C)
- Fig. S8 Fourier-transformed EXAFS data of samples taken from the quenched solutions at different stages of the synthesis process conditioned at (A). 10 mM H<sub>2</sub>PtCl<sub>6</sub>, 110 mM NaNO<sub>3</sub>, 160°C; (B). 5 mM H<sub>2</sub>PtCl<sub>6</sub>, 5 mM Fe(NO<sub>3</sub>)<sub>3</sub>, 140°C; (C). 5 mM H<sub>2</sub>PtCl<sub>6</sub>, 140°C.
- Fig. S9 Schematic illustration of the size and shape control of Pt NCs by the iron nitrate modified polyol process
- Fig. S10 ORR polarization curves recorded at room temperature in an O<sub>2</sub>-saturated 0.5 M HClO<sub>4</sub>

solution with a sweep rate of 20 mV/s and a rotation rate of 1,600 rpm. The current densities were normalized against the geometric area of the electrode (0.196 cm<sup>2</sup>)

Fig. S11 XRD patterns of commercial Pt black, the crystalline size is 7.7nm based on the Scherrer equation

Table S1 Summary of Pt NCs synthesized at 160°C for 20 min with different Fe/Pt ratio

Table S2 Summary of Pt NCs synthesized at different temperatures with the same Fe/Pt ratio

Table S3 Summary of Pt NCs synthesized at 140°C for 3 h with different Fe/Pt ratio

## Materials and chemicals

Ferric nitrate enneahydrate ( $\text{Fe}(\text{NO}_3)_3 \cdot 9\text{H}_2\text{O}$ ), ferric chloride hexahydrate ( $\text{FeCl}_3 \cdot 6\text{H}_2\text{O}$ ), sodium nitrate ( $\text{NaNO}_3$ ), copper nitrate ( $\text{Cu}(\text{NO}_3)_2 \cdot 3\text{H}_2\text{O}$ ) and ethylene glycol (EG) were of analytical grade and were obtained from Tianjin Kermel Co. in China. Dihydrogen hexachloroplatinate ( $\text{H}_2\text{PtCl}_6 \cdot 6\text{H}_2\text{O}$ , 99.9%, metal basis) and poly(vinylpyrrolidone) (PVP,  $M_w = 58000$ ) were purchased from Sigma. All the chemicals were used as received without further purification.

## Experiment

### 1. Preparation of monomorphic Pt tripod and octapod NCs

In a typical synthesis, 0.65 mL 77.22 mM  $\text{H}_2\text{PtCl}_6$  solution was rapidly added to 9.35 mL EG (held at 128°C, 140°C, 160°C, 180°C, respectively) which contained both 0.2 mL  $\text{Fe}(\text{NO}_3)_3$  solution at certain concentrations and 15 mM PVP (as calculated in terms of the repeating unit). The concentration of  $\text{H}_2\text{PtCl}_6$  was fixed at 5 mM for all the synthesis; the concentration of PVP was always fixed at 15 mM. While the concentration of  $\text{Fe}(\text{NO}_3)_3$  was varied in the range of 0 to 16 mM. In this so-called iron nitrate modified polyol synthesis, EG serves as both solvent and reducing agent.

**For tripod Pt NCs synthesis:** 0.65 mL 77.22 mM  $\text{H}_2\text{PtCl}_6$  solution was rapidly added to 9.35 mL EG being held at 128°C which contained 5 mM  $\text{Fe}(\text{NO}_3)_3$  and 15 mM PVP, and the mixed solution was stirring at 128°C for 3 h, then the solution was cooled down to room temperature, centrifuged, washed, and dispersed in ethanol for characterization.

**For octapod Pt NCs synthesis:** 0.65 mL 77.22 mM  $\text{H}_2\text{PtCl}_6$  solution was rapidly added to 9.35 mL EG being held at 140°C which contained 5 mM  $\text{Fe}(\text{NO}_3)_3$  and 15 mM PVP, and the mixed solution was stirring at 140°C for 3 h, then the solution was cooled down to room temperature, centrifuged, washed, and dispersed in ethanol for characterization.

### 2. Preparation of morphology controlled Pt NCs at various experimental conditions

Fig. S1 shows typical TEM images of Pt NCs that were obtained with the same Pt concentration of 5 mM but with different Fe/Pt ratio at the fixed temperature 160°C. These images clearly indicated the transformation in morphology as the Fe/Pt ratio was gradually increased. Crystals synthesized without the presence of Fe(NO<sub>3</sub>)<sub>3</sub> were irregular in shape and their sizes varied on the scale of 2-4.5 nm (Fig. S1a). With increasing iron nitrate concentration, Pt nanocrystal size increased and morphologies became rich as shown in Table S1. The morphology of tripod and octapod appeared when the concentration of Fe(NO<sub>3</sub>)<sub>3</sub> was high enough, however, only a mixture of tripod and octapod NCs was produced. But it was believed that through the modification of synthesis parameters it was possible to observe the monomorphic tripod or octapod Pt NCs. Temperature is a very important parameter in the polyol process. Here the Fe/Pt ratio and Pt concentration were fixed, the morphology variation of Pt NCs with decreasing temperature was observed shown in Fig. S2. It is very interesting that the growth trend of the ridges of NCs is much more obvious with decreasing the temperature as summarized in Table S2. When the temperature was as low as 128°C, the nanostructure of tripod occupied the most parts about 82.1% given in the Fig. 1a. When the temperature increased to 140°C, almost monomorphic structure of octapod could be obtained which occupied about 92.8% as shown in Fig. 1b. As the temperature increased to 160°C, truncated cube appeared. And when the temperature was as high as 180°C, the shape of crystals became sphere. This trend is in accord with the reported mechanism that the morphology evolution was controlled by the reduction kinetics of the Pt precursor. These results indicated that reduction temperature could be used to control the morphology of the Pt NCs. When the temperature was high, the reduction process was relatively fast, so the nanocrystallite seeds tended to grow into the thermodynamically favoured shape such as sphere in order to minimize the surface energy. Otherwise when the temperature was much low, the reduction rate was greatly slowed down resulting in the overgrowth of certain ridges of Pt NCs.

TEM images of Pt NCs synthesized at 160°C but with the different Fe/Pt ratio are shown earlier.

At 160°C, the crystal size increases and the morphology becomes rich with increasing the Fe/Pt ratio. According to the reduction kinetics it is believed that the morphologies will be richer if the temperature is some low with the fixed Fe/Pt ratio. Fig. S3 shows TEM images of Pt NCs synthesized at 140°C with the same H<sub>2</sub>PtCl<sub>6</sub> concentration (5 mM) but different Fe/Pt ratio. From the summarized Table S3, with increasing Fe/Pt ratio the reduction rate was much more greatly slowed down, so overgrowth of Pt seeds dominated the growth step. Then it resulted in the formation of large NCs with a large number of edge, corner, and surface step atoms in high yield such as tripods, octapods, pentapods, and needle type of multipods. In a typical polyol process synthesis, the concentration of H<sub>2</sub>PtCl<sub>6</sub> also played an important role in the morphology of Pt NCs. As shown as in Fig. S4, with decreasing the concentration of H<sub>2</sub>PtCl<sub>6</sub>, the Pt nanostructures transformed from octahedron to octapod when the Fe/Pt ratio was fixed at 1 and the temperature was fixed at 140°C, there were no much differences in the sizes of Pt NCs.

### 3. Electrochemical measurements

Electrochemical measurements were performed using a glassy carbon rotating disk electrodes (RDE) connected to a potentiationstat. A hydrogen reference electrode was used, and the counter electrode was a platinum mesh (1 cm × 1 cm) attached to a platinum wire. To prepare the working electrode, the sample was washed with water/acetone and ethanol/acetone solutions for at least 5 times respectively and dispersed in ethanol then diluted to 0.15 μgμL<sup>-1</sup> (based on inductively coupled plasma (ICP)-MS measurements) and 65.3 μL of the dispersion was transferred onto the glassy carbon RDE with a geometric area of 0.196 cm<sup>2</sup>. The loading amount of Pt for all catalysts was 50 μgcm<sup>-2</sup>. After evaporation of ethanol, the electrode was coated with 20 μL of 0.025 wt% Nafion solution.

Cyclic voltammetry (CV) measurements were carried out in 0.5 molL<sup>-1</sup> HClO<sub>4</sub> solutions under a flow of N<sub>2</sub> (Airgas, ultrahigh purity) at a sweep rate of 20 mVs<sup>-1</sup>. The ECSA was estimated by measuring the charges associated with H<sub>upd</sub> adsorption/desorption (Q) between 0.05 and 0.40 V

after double-layer correction and assuming a value of  $210 \mu\text{C cm}^{-2}$  for the adsorption of a monolayer of hydrogen onto a Pt surface ( $q_{\text{H}}$ ). Then, the specific ECSA was calculated based on the following relation:  $\text{specific ECSA} = 0.5Q / (mq_{\text{H}})$ , where  $Q$  is the charge associated with  $\text{H}_{\text{upd}}$  adsorption or desorption,  $m$  is the mass of loaded metal, and  $q_{\text{H}}$  is the charge required for the adsorption of a monolayer of hydrogen on a Pt surface.

The ORR measurements were conducted at room temperature in 0.5 M  $\text{HClO}_4$  solutions under a flow of  $\text{O}_2$  using the glassy carbon RDE at a rotation rate of 1600 rpm and a sweep rate of  $20 \text{ mVs}^{-1}$ .

The kinetic current was calculated based on the Koutecky–Levich equation:

$$\frac{1}{i} = \frac{1}{i_k} + \frac{1}{i_d}$$

where  $i$  is the experimentally measured current,  $i_d$  is the diffusion limiting current, and  $i_k$  is the kinetic current. For each catalyst, the kinetic current was normalized to ECSA in order to obtain specific activities.

#### 4. Nanocrystal characterizations

Transmission electron microscope (TEM) were carried out using a Tecnai G2 Spirit FEI transmission electron microscope operating at 120 kV. High-resolution transmission electron microscope (HRTEM) were carried out using Tecnai G2 F30 S-Twin Transmission Electron Microscope, operating at 300 kv. A few droplets of a suspension of one sample in ethanol were put on a micro-grid carbon polymer supported on a nickel grid. The samples for TEM and HRTEM characterization were prepared by depositing a drop of dilute sample solution on a carbon-coated copper grid and dried at room temperature.

X-ray diffraction (XRD) patterns were collected on a PW3040/60 X' Pert PRO (PANalytical) diffractometer equipped with a Cu KR radiation source ( $\lambda = 0.15432 \text{ nm}$ ).

UV/Vis absorption spectra were recorded using a Cintra (GBC) apparatus. 40  $\mu\text{L}$  of the sampled solution was then diluted with 3 mL ethanol for UV/Vis spectral measurements.

The Pt-L<sub>III</sub> edge and Fe-K edge EXAFS (extended X-ray absorption fine structure spectroscopy)

measurements over the quenched solutions were carried out at the BL14W1 beamline of SSRF, SINAP (Shanghai, China), with the use of a Si (111) crystal monochromator. The electron storage ring is 3.5 GeV and a stored beam current of 140-210 mA. Pt foil, PtO<sub>2</sub>, H<sub>2</sub>PtCl<sub>6</sub> solution, Fe foil, Fe(NO<sub>3</sub>)<sub>3</sub> solution and FeSO<sub>4</sub> solution were used as reference samples, respectively, and the X-ray absorption spectra of Pt foil, PtO<sub>2</sub> and Fe foil were measured in the transmission mode at room temperature. All the other spectra were collected in fluorescence mode at room temperature. Energy was scanned from 200 eV below the edge to 1000 eV above the edge. The raw data were energy-calibrated (Pt-L<sub>III</sub> edge energy of Pt foil 11564 eV, Fe-K edge energy of Fe foil 7112 eV, first inflection point), background-corrected, and normalized using the IFEFFIT software. Fourier transformation of the XAFS data was applied to the k<sup>2</sup>-weighted functions, respectively.

Electrochemical test was carried out on a chi 760 potentiationstat.

The amount of Pt catalyst used in each sample for electrochemical measurements were determined by inductively coupled plasma spectrometer (ICP-AES) on an IRIS Intrepid II XSP instrument (Thermo Electron Corporation).

## 5. The PVP Effect

In order to open out the function of PVP used as the capping agent in the synthesis, CTAB was applied for a comparison in the present process of the Pt NCs preparation. According to the literature, PVP acts as a stabilizing agent, preventing aggregation of metal particles and retaining a uniform colloidal dispersion. Spectroscopic studies indicate that the PVP-metal interaction occurs through the carbonyl group of the pyrrolidone ring. This interaction has been empirically shown to be quite strong, with PVP replacement occurring only by the formation of a self-assembled monolayer of alkanethiol. If PVP was not used in the synthesis process, the particles aggregated heavily as shown in Fig. S5. It is recognized that nanoparticles tended to agglomerate and settle down in the solution without capping agent. The CTAB is different from PVP; it has a very weak interaction with the metal. When CTAB was applied as a capping agent, under the same conditions

as in Fig. 2b, the obtained particles aggregated strongly as shown as in Fig. S5. So it is believed that preventing the fast reduction of metal ions and aggregation – especially for colloidal syntheses carried out at high temperatures – is necessary for the successful preparation of monodisperse metal NCs. So as a surface-capping agent, it must have a strong interaction with the metal to prevent the particles aggregation for colloidal syntheses carried out at high temperatures. In all the synthesis process, the concentration of PVP was fixed. So the morphology was controlled by the reduction kinetics with changing the temperature and concentration of the oxidative etchants during the synthesis process.

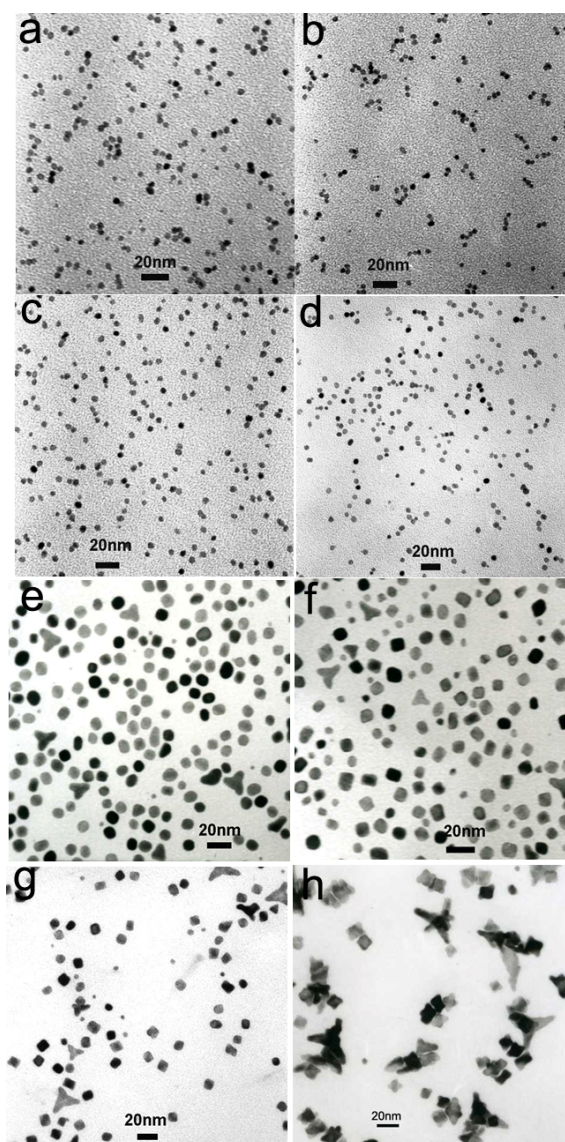


Fig. S1 TEM images of Pt NCs synthesized at 160°C for 20 min with different ratios between  $\text{Fe}(\text{NO}_3)_3$  and  $\text{H}_2\text{PtCl}_6$  (a) 0, (b) 0.02, (c) 0.1, (d) 0.2, (e) 0.4, (f) 1.0, (g) 1.2, (h) 1.6

**Table S1** Summary of Pt NCs synthesized at 160°C for 20 min with different Fe/Pt ratio

| Sample   | Fe/Pt | $C_{\text{Pt}}$ (mM) | T (°C) | Size (nm) | Shape   |
|----------|-------|----------------------|--------|-----------|---|
| Pt       | 0     | 5                    | 160    | 3.3       |    |
| Pt5Fe0.1 | 0.02  | 5                    | 160    | 3.4       |    |
| Pt5Fe0.5 | 0.1   | 5                    | 160    | 4.1       |    |
| Pt5Fe1   | 0.2   | 5                    | 160    | 5.3       |    |
| Pt5Fe2   | 0.4   | 5                    | 160    | 7.4       |     |
| Pt5Fe5   | 1     | 5                    | 160    | 9.8       |     |
| Pt5Fe6   | 1.2   | 5                    | 160    | 10        |    |
| Pt5Fe8   | 1.4   | 5                    | 160    | 15        |     |

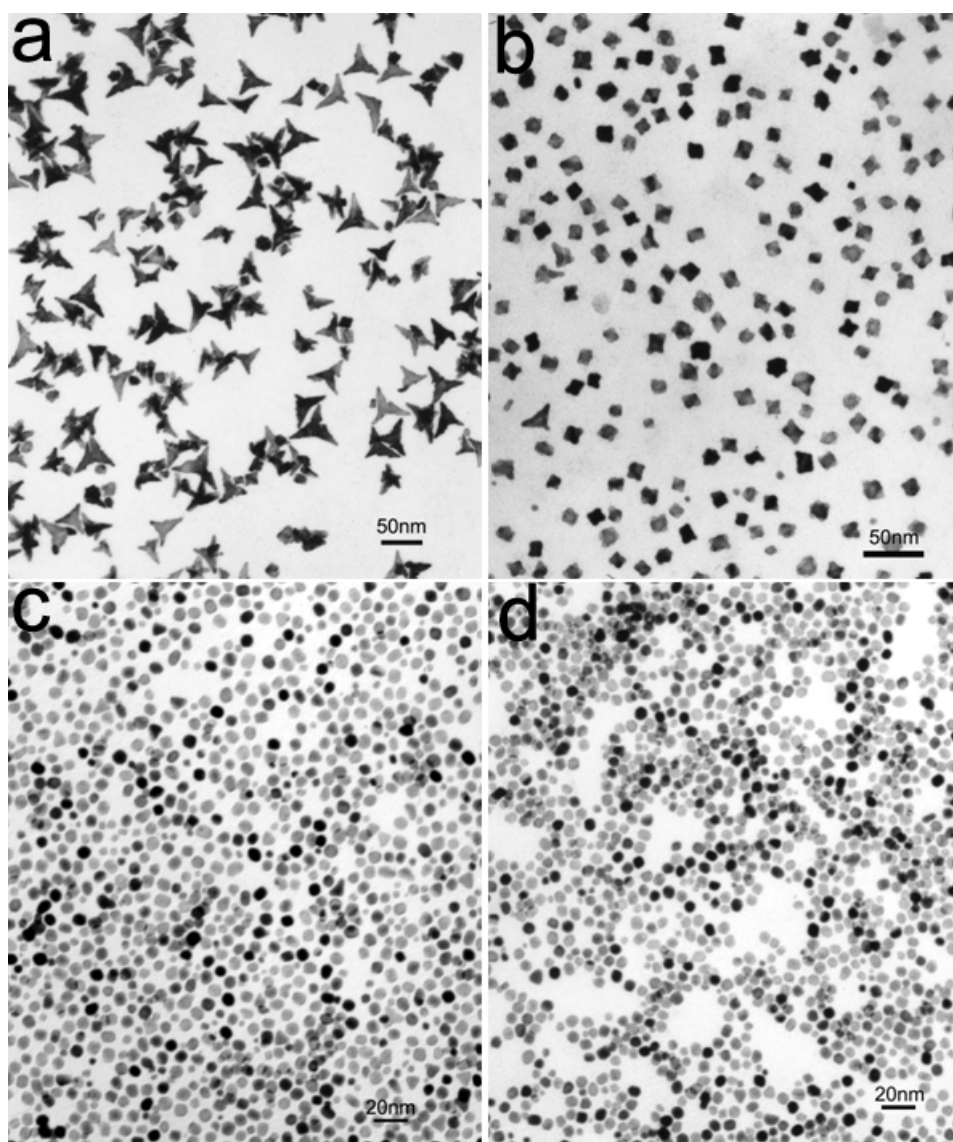


Fig. S2 TEM images of Pt/Pt NCs synthesized at 5 mM  $\text{H}_2\text{PtCl}_6$  and 5 mM  $\text{Fe}(\text{NO}_3)_3$  with different temperatures (a)128°C, (b)140°C, (c)160°C, (d)180°C for 3 h

**Table S2** Summary of Pt NCs synthesized at different temperatures with the same Fe/Pt ratio

| Sample | Fe/Pt | $C_{\text{Pt}}$ (mM) | T(°C) | Size (nm) | TEM   | Shape   |
|--------|-------|----------------------|-------|-----------|---|---|
| Pt5Fe5 | 1     | 5                    | 128   | 15        |  |  |
| Pt5Fe5 | 1     | 5                    | 140   | 10        |  |  |
| Pt5Fe5 | 1     | 5                    | 160   | 7         |  |  |
| Pt5Fe5 | 1     | 5                    | 180   | 6         |  |  |

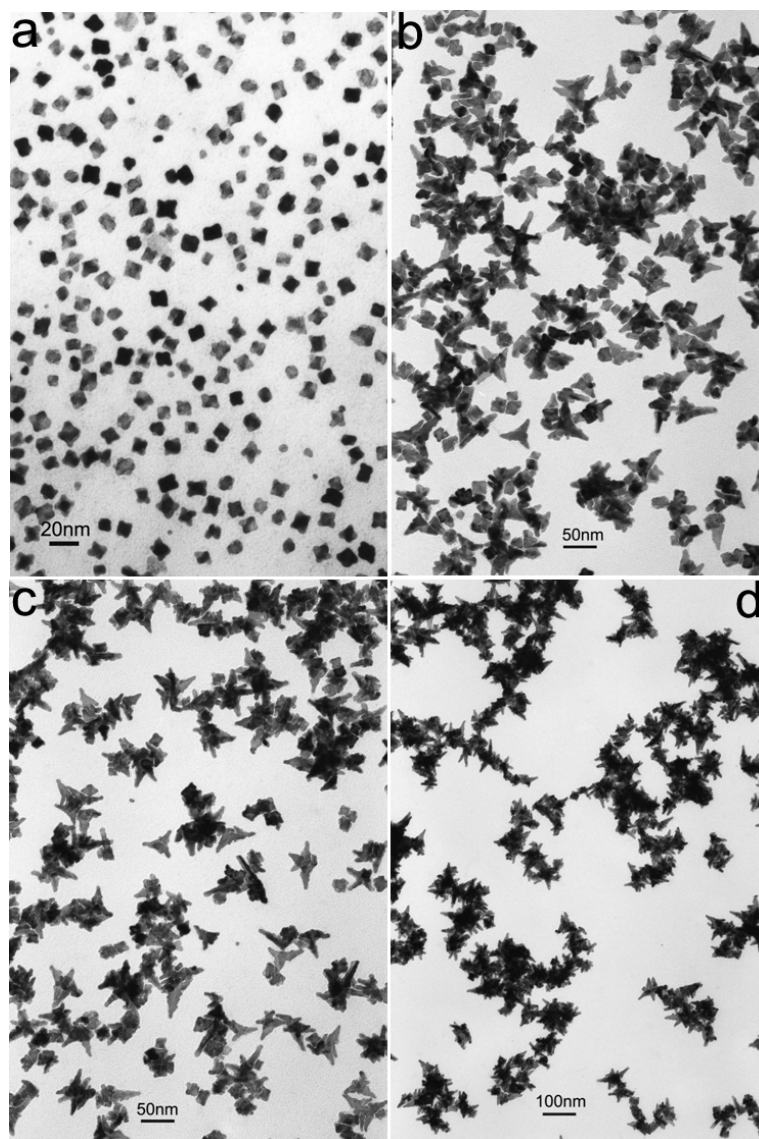


Fig. S3 TEM images of Pt NCs synthesized at the same temperature (140°C) and the same Pt concentration (5 mM) but with different ratios between  $\text{Fe}(\text{NO}_3)_3$  and  $\text{H}_2\text{PtCl}_6$  (a) 1.0, (b) 1.2, (c) 1.8, (d) 2.0 for 3 h

**Table S3** Summary of Pt NCs synthesized at 140°C for 3 h with different Fe/Pt ratio

| Sample  | Fe/Pt | $C_{\text{Pt}}$ (mM) | T(°C) | Size (nm) | TEM | Shape |
|---------|-------|----------------------|-------|-----------|-----|-------|
| Pt5Fe3  | 0.6   | 5                    | 140   | 11        |     |       |
| Pt5Fe5  | 1     | 5                    | 140   | 10        |     |       |
| Pt5Fe7  | 1.4   | 5                    | 140   | ~ 20      |     |       |
| Pt5Fe8  | 1.6   | 5                    | 140   | ~30       |     |       |
| Pt5Fe10 | 2     | 5                    | 140   | ~50       |     |       |

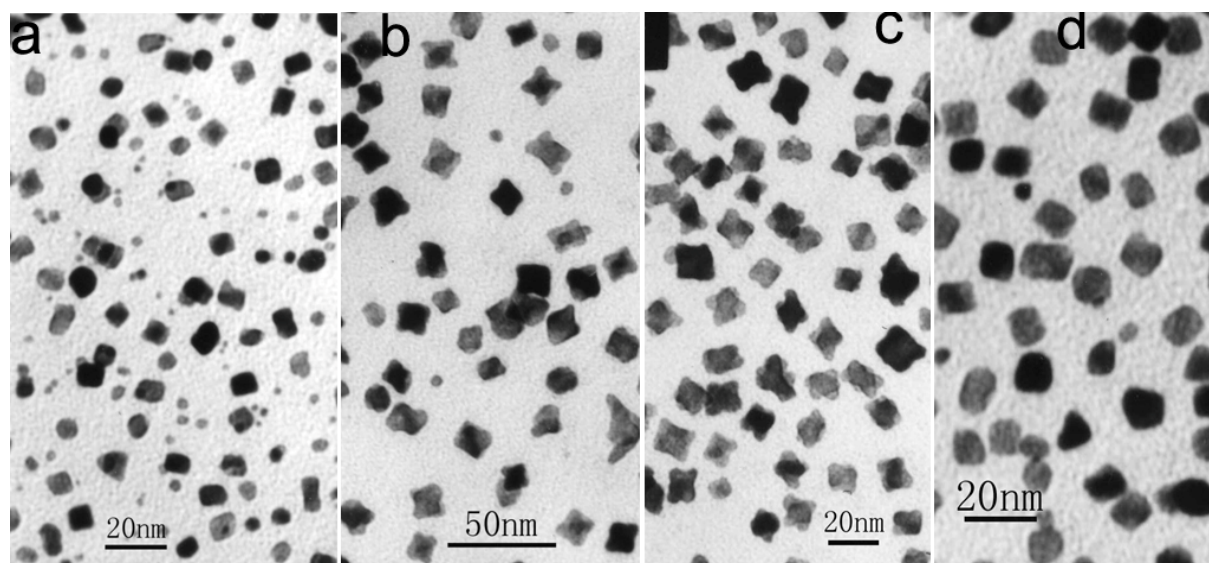


Fig. S4 TEM images of Pt NCs synthesized at the same temperature (140°C) with same ratios between  $\text{Fe}(\text{NO}_3)_3$  and  $\text{H}_2\text{PtCl}_6$  but at different Pt concentrations (a) 3 mM, (b) 4 mM, (c) 5 mM, (d) 6 mM, (e) 7 mM for 3 h

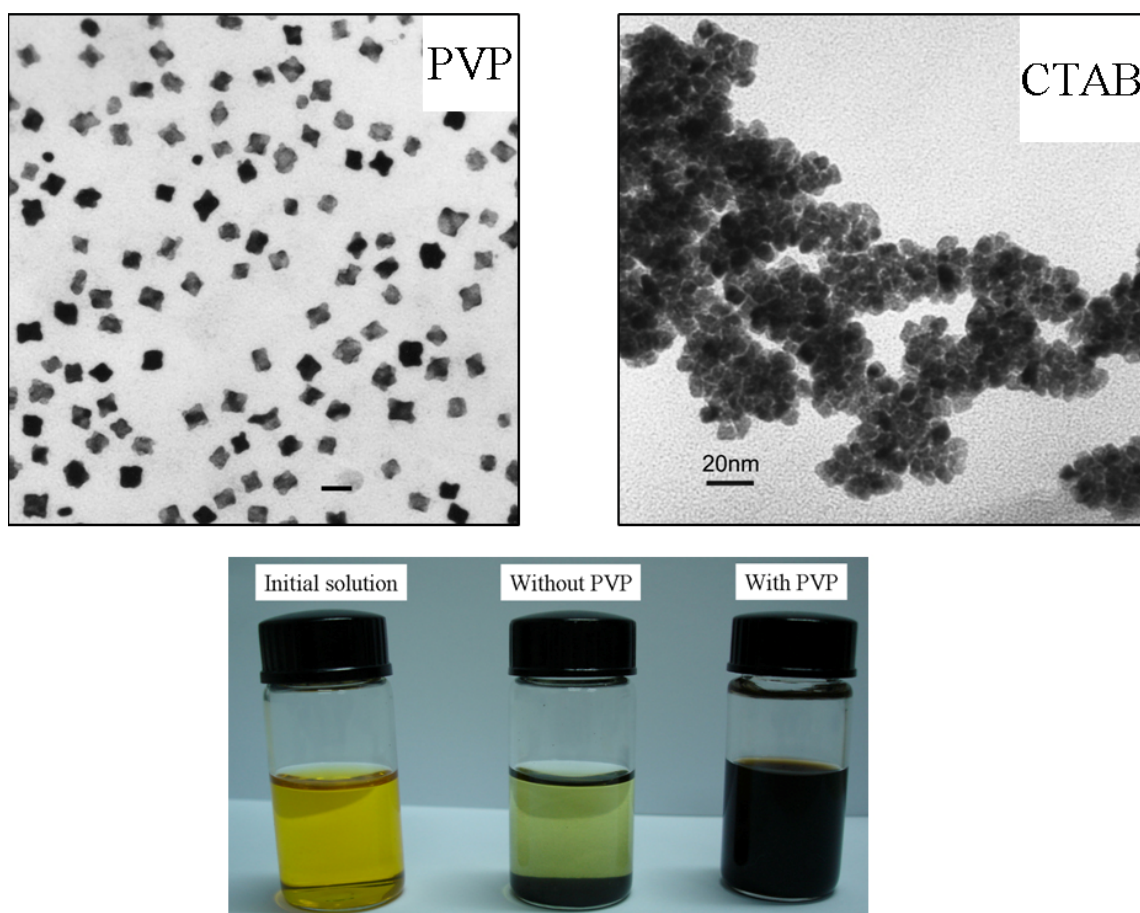


Fig. S5 TEM images of the Pt NCs prepared at 5 mM  $\text{H}_2\text{PtCl}_6$  and 5 mM  $\text{Fe}(\text{NO}_3)_3$  at  $140^\circ\text{C}$  with PVP and CTAB, respectively and pictures of the initial colloid solution and the product solutions with and without PVP

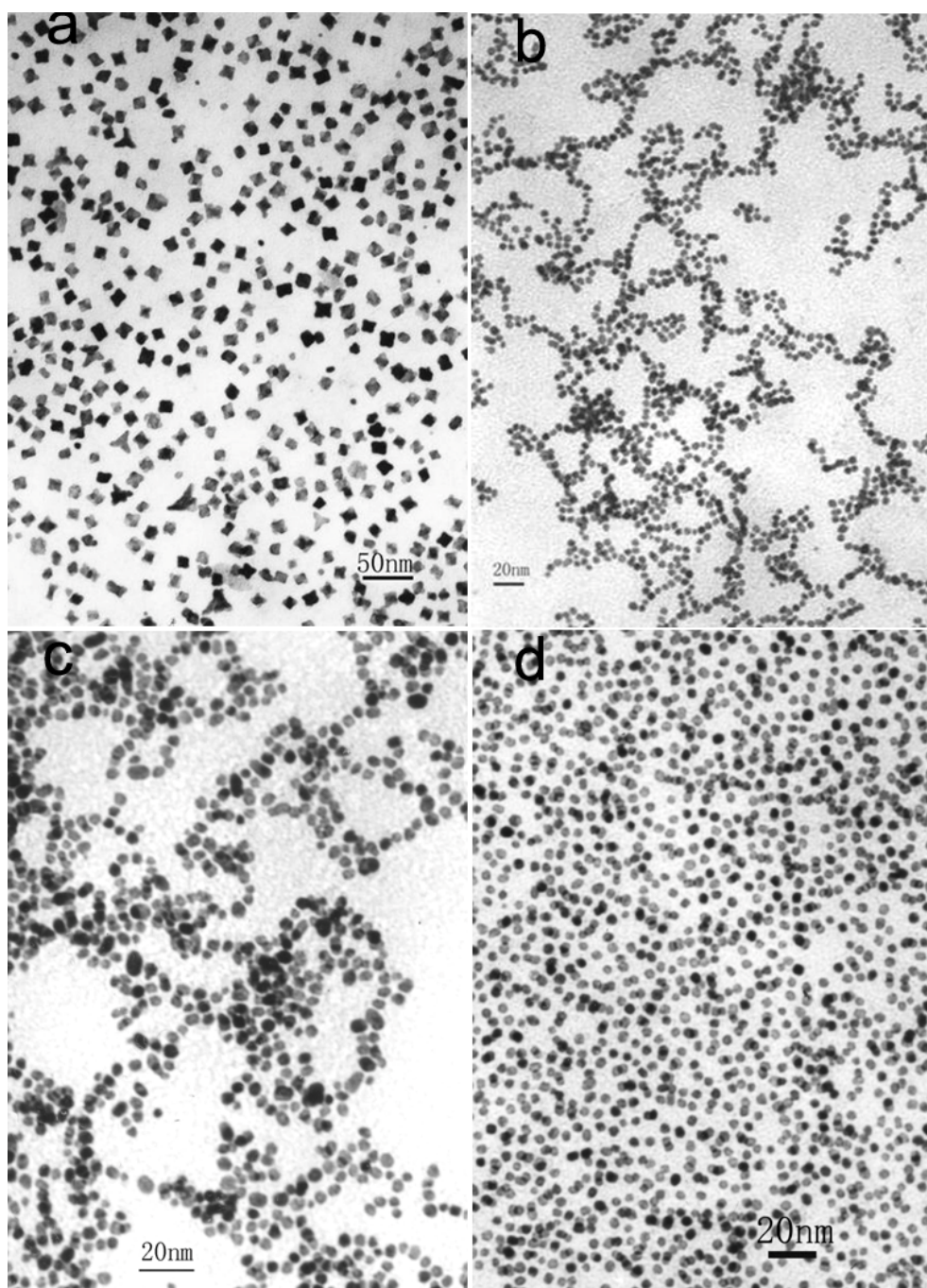


Fig. S6 TEM images of Pt NCs synthesized at the same temperature ( $140^{\circ}\text{C}$ ) and the same Pt concentration (5 mM) but with different modifier (a) 5 mM  $\text{Fe}(\text{NO}_3)_3$ , (b) 5 mM  $\text{FeCl}_3$ , (c) 15 mM  $\text{NaNO}_3$ , (d) 7.5 mM  $\text{Cu}(\text{NO}_3)_2$

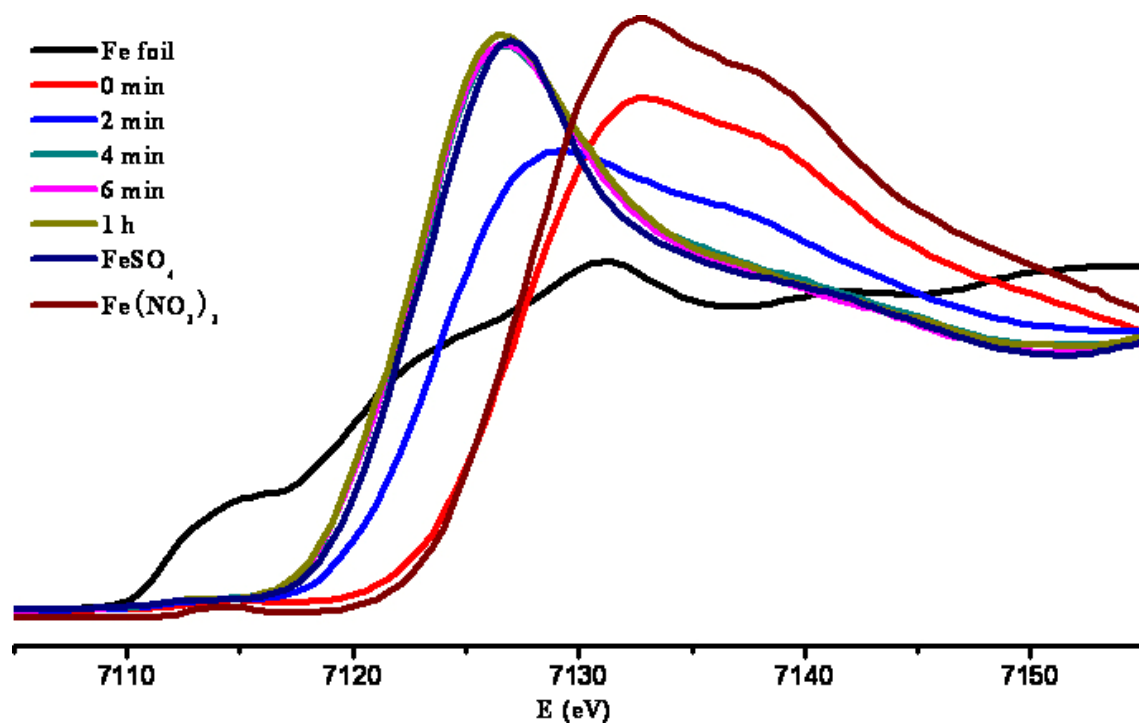


Fig. S7 X-ray absorption near-edge fine structure spectra of iron species taken from the quenched solutions at different stages of the synthesis process of Pt octapod (5 mM H<sub>2</sub>PtCl<sub>6</sub>, 5 mM Fe(NO<sub>3</sub>)<sub>3</sub>, 140°C)

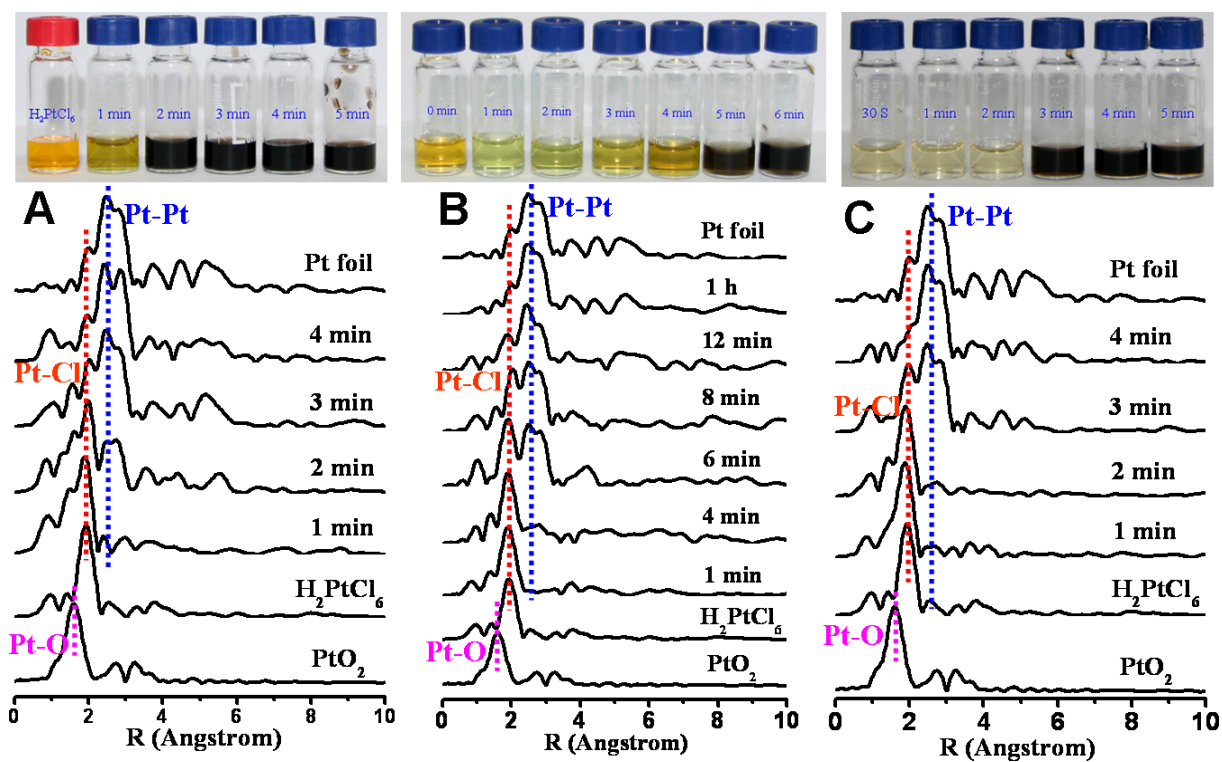


Fig. S8 Fourier-transformed EXAFS data of samples taken from the quenched solutions at different stages of the synthesis process conditioned at (A). 10 mM H<sub>2</sub>PtCl<sub>6</sub>, 110 mM NaNO<sub>3</sub>, 160°C; (B). 5 mM H<sub>2</sub>PtCl<sub>6</sub>, 5 mM Fe(NO<sub>3</sub>)<sub>3</sub>, 140°C; (C). 5 mM H<sub>2</sub>PtCl<sub>6</sub>, 140°C

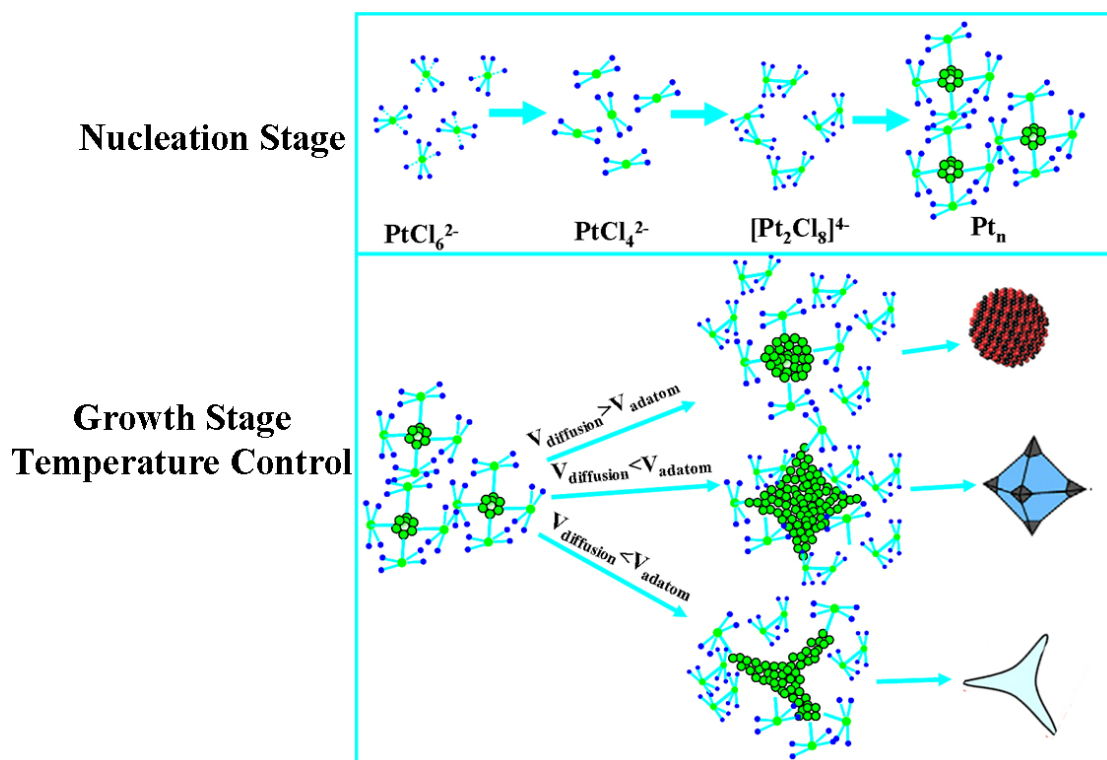


Fig. S9 Schematic illustration of the size and shape control of Pt NCs by the iron nitrate modified polyol process

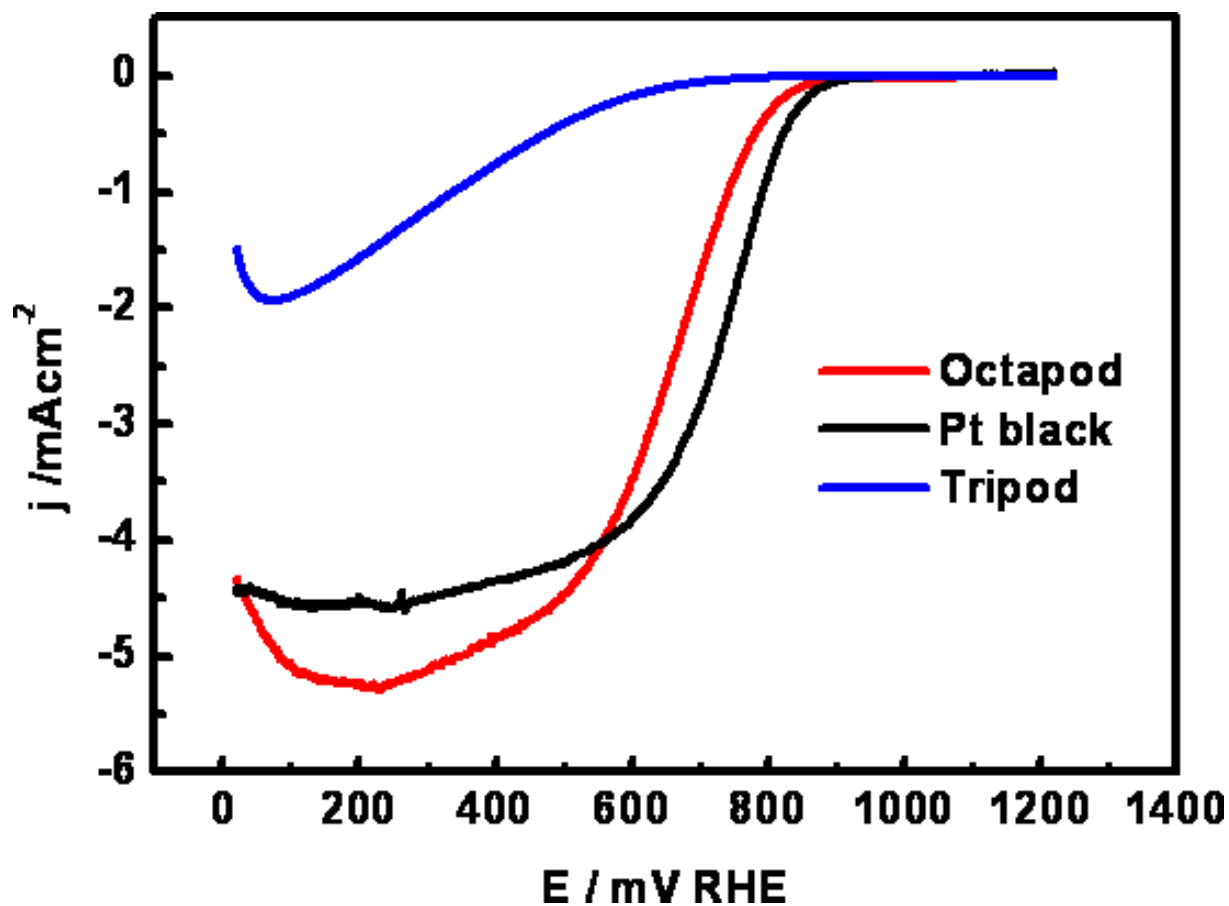


Fig. S10 ORR polarization curves recorded at room temperature in an  $\text{O}_2$ -saturated 0.5 M  $\text{HClO}_4$  solution with a sweep rate of 20  $\text{mV/s}$  and a rotation rate of 1,600 rpm. The current densities were normalized against the geometric area of the electrode ( $0.196 \text{ cm}^2$ )

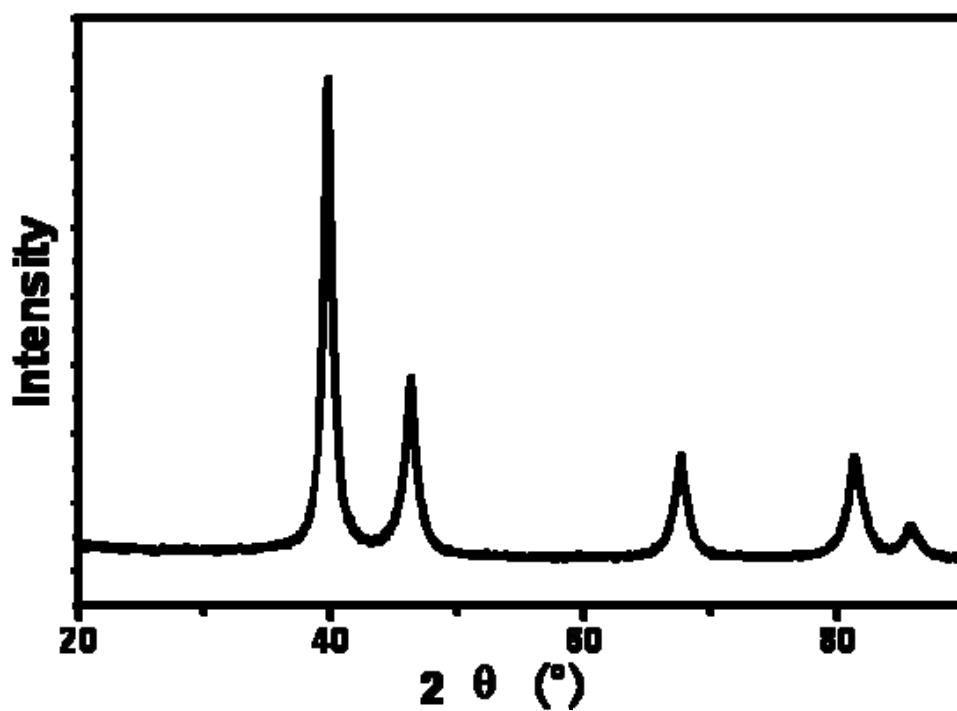


Fig. S11 XRD patterns of commercial Pt black, the crystalline size is 7.7nm based on the Scherrer equation